

Thermally excited capillary waves at vapor/liquid interfaces of water–alcohol mixtures

This article has been downloaded from IOPscience. Please scroll down to see the full text article.

2009 J. Phys.: Condens. Matter 21 115105

(<http://iopscience.iop.org/0953-8984/21/11/115105>)

View [the table of contents for this issue](#), or go to the [journal homepage](#) for more

Download details:

IP Address: 129.252.86.83

The article was downloaded on 29/05/2010 at 18:37

Please note that [terms and conditions apply](#).

Thermally excited capillary waves at vapor/liquid interfaces of water–alcohol mixtures

David Vaknin^{1,2}, Wei Bu^{1,2}, Jaeho Sung³, Yoonnam Jeon³ and Doseok Kim³

¹ Ames Laboratory, Iowa State University, Ames, IA 50011, USA

² Department of Physics and Astronomy, Iowa State University, Ames, IA 50011, USA

³ Department of Physics and Interdisciplinary Program of Integrated Biotechnology, Sogang University, Seoul 121-742, Korea

Received 3 December 2008

Published 2 February 2009

Online at stacks.iop.org/JPhysCM/21/115105

Abstract

The density profiles of liquid/vapor interfaces of water–alcohol (methanol, ethanol and propanol) mixtures were studied by surface-sensitive synchrotron x-ray scattering techniques. X-ray reflectivity and diffuse scattering measurements, from the pure and mixed liquids, were analyzed in the framework of capillary wave theory to address the characteristic length scales of the intrinsic roughness and the shortest capillary wavelength (alternatively, the upper wavevector cutoff in capillary wave theory). Our results establish that the intrinsic roughness is dominated by average interatomic distances. The extracted effective upper wavevector cutoff indicates capillary wave theory breaks down at distances of the order of bulk correlation lengths.

(Some figures in this article are in colour only in the electronic version)

1. Introduction

It is by now common theoretically [1–9] and experimentally [10–20] that the density profile of simple liquid/vapor interfaces is dominated by thermally excited capillary waves. Theoretically, the profile is derived by statistical mechanics tools assuming thermal excitations in a two-dimensional membrane under surface tension and under the influence of gravity on mass displacements. Initially, the density profiles were measured in the vicinity of the critical point of liquids, where the interfacial profile is sufficiently wide (i.e. very low surface tension) to be adequately resolved by light scattering techniques [10, 11]. However, with the advent of the x-ray scattering technique for liquid surfaces [21], the profiles of common simple liquids, such as water and alcohols, away from the critical point have been determined to be a few ångströms thick [12].

The x-ray reflectivity from a liquid surface $R(q_z)$ ($q_z = 2k_0 \sin \alpha$; α incident beam angle, $k_0 = 2\pi/\lambda$; λ x-ray wavelength; see inset in figure 1) is given by [12, 15, 20, 22, 23]

$$R(q_z) = R_F(q_z)R(0, q_z)e^{-\sigma_0^2 q_z^2} \quad (1)$$

where $R_F(q_z)$ is the Fresnel reflectivity from an ideally flat surface, σ_0 is the intrinsic roughness and for a

rectangular-shaped resolution function (used in the present experiment) [22]:

$$R(0, q_z) = \frac{2^{1-2\eta}\Gamma(1/2 - \eta/2)}{\sqrt{\pi}\eta\Gamma(\eta/2)} \left(\frac{\Delta q_y}{q_{\max}}\right)^\eta \quad (2)$$

where $\eta = \frac{k_B T}{2\pi\gamma} q_z^2$ and $\Delta q_y = q_z \Delta\beta/2$. Here, $\Delta\beta$ is the detector acceptance angle, γ is the surface tension and T is the sample temperature. In the q_z range of a typical reflectivity measurement, η values are small and we can use the following expression:

$$R(q_z)/R_F \approx e^{(-\sigma_{\text{cw}}^2 - \sigma_0^2)q_z^2} = e^{-\sigma_{\text{eff}}^2 q_z^2}, \quad (3)$$

where the effective roughness can be written as follows [12, 14, 16, 18, 20]:

$$\sigma_{\text{eff}}^2 \equiv \sigma_0^2 + \sigma_{\text{cw}}^2 = \sigma_0^2 + \frac{k_B T}{2\pi\gamma} \ln\left(\frac{q_{\max}}{q_{\min}}\right), \quad (4)$$

where σ_{eff} depends on q_z and $\Delta\beta$ from the relation $q_{\min} = q_z \Delta\beta/2$.

It has been suggested that the intrinsic roughness σ_0 scales with molecular size, and q_{\max} in equation (4) has

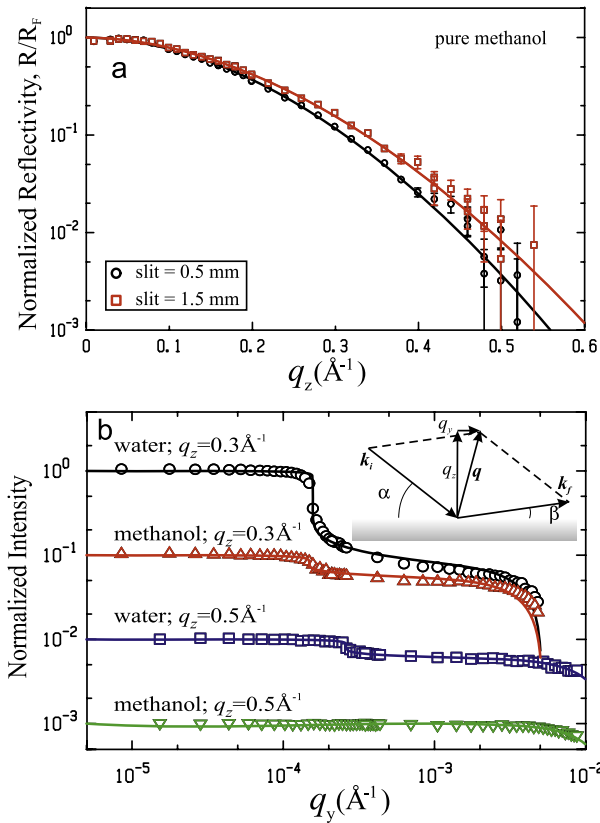


Figure 1. (a) Normalized x-ray reflectivities of pure methanol versus q_z demonstrating the effect of the resolution on the measurement (detector slit sizes indicated). The solid lines were obtained by simultaneous fitting using equation (3). (b) The XDS from pure water and pure methanol at constant q_z values as indicated (shifted by a decade each for clarity). The solid lines are fits to the data using equation (5). The inset shows the experimental beam geometry.

been usually estimated from the molecular size R such that $q_{\max} = \pi/R$ [12]. However, studies of pure water and pure ethanol [14, 15] found $\sigma_0 = 0$, implying a perfectly uniform electron density with no atomic or molecular discreteness of the liquid. It should be noted that, in the studies mentioned above, the contributions of σ_0 and q_{\max} to the surface roughness according to equation (4) could not be decoupled⁴. Subsequently, in a study of long-chain C20 and C36 alkanes, by varying the liquid temperature, it was found that $\sigma_0 = 1.1 \text{ \AA}$, significantly smaller than the molecular size [16].

In the present study we employ synchrotron x-ray reflectivity studies to determine the relevant parameters of capillary wave theory, i.e. σ_0 , q_{\min} and q_{\max} , by systematically varying the surface tension of simple alcohols (methanol, ethanol and propanol) and their mixtures with water. The alcohol molecules are very close in size to a water molecule (in particular methanol), thus minimizing the presumed differences due to molecular size through σ_0 or q_{\max} , yet allowing the continuous variation of surface tension over a

⁴ Equation (4) can be written as follows: $\sigma_{\text{eff}}^2 = [\sigma_0^2 + \frac{k_B T}{2\pi\gamma} \ln(q_{\max})] - \frac{k_B T}{2\pi\gamma} \ln(q_z \Delta\beta/2)$ showing the contributions of σ_0 and q_{\max} cannot be decoupled by varying the slit size, but only by varying temperature and/or surface tension.

wide range (22–73 mN m⁻¹ at room temperature) by changing the mixture concentration [24].

2. Experimental details

The alcohols (methanol 99.9%, ethanol 99.5% and 1-propanol 99.5%), purchased from Fisher Chemicals, were used without further purification. Ultrapure water (Millipore, Milli-Q and NANOpure, Barnstead; resistivity, 18.1 M Ω cm) was used to make the mixtures, without any buffer to adjust the pH (pH \sim 6.5). The surface tension of all solutions was measured at 21 $^\circ$ C using a DuNuoy Tensiometer. X-ray reflectivity measurements were conducted on the Ames Laboratory Liquid Surface Diffractometer, in sector 6 of the Advanced Photon Source (APS) at Argonne National Laboratory [25, 26]. The highly monochromatic beam (16.2 keV was used for all liquids and mixtures and 8 keV for water/propanol mixtures), selected by a downstream Si double-crystal monochromator, is deflected onto the liquid surface to a desired angle of incidence (α) with respect to the liquid surface by a second monochromator located on the diffractometer. The trough containing the liquid samples (\approx 10 cm in diameter and \sim 200 μ m deep) is enclosed inside a temperature-controlled and gas-tight aluminum canister. A thin liquid film approximately 200–300 μ m deep, an active vibration isolation unit (JAS Mod-2) and a 3 s waiting time after the movement of any component of the diffractometer before counting photons, are used to obviate the effect of undesirable mechanical agitations of the liquid. Before the start of each measurement the shape (peak height and width) of the totally reflected beam below the critical angle is confirmed to be practically the same as that of the direct beam [25]. The volume enclosing the trough is constantly purged with helium bubbled through the corresponding water/alcohol mixture.

3. Results and discussion

As shown in equation (4), the effective surface roughness depends on the instrumental resolution via q_{\min} . To validate the resolution of our experimental set-up, we conducted x-ray reflectivity (XR) from pure methanol under two detector slit conditions, as shown in figure 1(a). The 0.5 and 1.5 mm detector slit widths at a distance of 756 mm from the sample center yield $\Delta\beta \approx 0.00066$ and 0.0020 rad, respectively. The nonlinear least-squares fit to the data using equation (3) (solid lines) with the logarithmic dependence on q_z yields $\sigma_{\text{eff}} = 4.9_{-0.2}^{+0.1}$ (for the 0.5 mm slit) and $4.55_{-0.14}^{+0.13}$ \AA (for the 1.5 mm slit) at $q_z = 0.3 \text{ \AA}^{-1}$. Detailed analysis shows that σ_0 can take values from $\sigma_0 = 0$ to σ_{eff} by allowing q_{\max} to vary without any constraints (see footnote 4). In addition, as pointed out in [18], the logarithmic dependence of σ_{eff} on q_z is so weak that using a constant σ'_{eff} yields similar results as for q_z -dependent σ_{eff} (at a midpoint in the measured q_z range; $q_z \approx 0.3 \text{ \AA}^{-1}$). Indeed, this simpler approach gives within uncertainties the same result ($\sigma'_{\text{eff}} = 4.90 \pm 0.13$ and $4.59 \pm 0.13 \text{ \AA}$ (for the 0.5 and 1.5 mm slits, respectively)) as the one that assumes q_z -dependent σ_{eff} .

To further examine resolution effects and the contribution of capillary waves, we measured x-ray diffuse scattering (XDS) for water and methanol under the same slit conditions

used to obtain XR data (detector slit at 1.5 mm). In the past, the XDS from water and other liquids [14, 15, 18–20] has been thoroughly investigated, confirming capillary wave predictions. However, similar to specular reflectivity data, only σ_{eff} can be determined whereas the values of σ_0 and q_{max} can be decoupled only if the temperature and/or surface tension are varied. To a good approximation our resolution function is rectangular (incident-beam-slit ≈ 0.08 mm and beam divergence $\sim 10^{-5}$ rad). Following the detailed procedure in [20, 22], and by defining $I(q_y, q_z) = I_m(q_y, q_z) \sin \alpha / |T(\alpha)|^2 |T(\beta)|^2$, where the I_m is the measured intensity and $T(\alpha)$, $T(\beta)$ are the transmission functions, we find the normalized XDS is [23]

$$\frac{I(q_y, q_z)}{I(0, q_z)} = Cg(\alpha, \beta) + (1 - Cg_0) \times \frac{(\Delta q_y - 2q_y)|\Delta q_y - 2q_y|^{\eta-1} + (\Delta q_y + 2q_y)|\Delta q_y + 2q_y|^{\eta-1}}{2(q_z \Delta \beta / 2)^\eta}, \quad (5)$$

where $\Delta q_y = (q_z^2 - 2k_0 q_y) / (2q_z \Delta \beta)$, $g(\alpha, \beta) = D(\alpha)D(\beta) / (D(\alpha) + D(\beta))$ (D is the x-ray penetration depth), $g_0 = g(\alpha, \alpha)$ accounts for scattering from the bulk structure factor and C is a constant determined experimentally at a small azimuthal angle away from the scattering plane for the specular reflectivity condition [20, 23]. Figure 1(b) shows XDS measurements for water and methanol at fixed q_z (i.e. varying $q_y = k_0(\cos \beta - \cos \alpha)$ by changing α and β such that $\sin(\alpha) + \sin(\beta) = q_z / 2k_0$ is constant) normalized to the measured reflectivity at $q_y = 0$. By normalizing the XDS data, the two coupled parameters, σ_0 and q_{max} , are eliminated (see footnote 4). The calculated intensity to the normalized data (solid lines) using equation (5) with no adjustable parameters confirms the XDS are accounted for by capillary waves and also confirms the instrumental q_{min} value.

Figure 2 shows the normalized reflectivities of the pure liquids as indicated. Whereas the reflectivity of water is significantly different, the reflectivities of all three alcohols are hardly distinguishable. Since surface tension of the alcohols are very close in value, σ_{cw} is practically the same for all three, indicating the intrinsic roughness (σ_0) is not dominated by molecular size. Three different procedures for analyzing the data in figure 2 were examined. In the first (dotted lines), we assume that the only free parameter in equation (3) is σ_0 and fixed $q_{\text{max}} = \pi/R$, where R is the average radius of each molecule: 1.93, 2.52, 2.85 and 3.1 Å for water, methanol, ethanol and propanol, respectively. All the fits (dotted lines) yielded $\sigma_0 \approx 0$ and, except for water, the fit is very poor. By relaxing the constraint on q_{max} we get a better fit to the data (solid lines) with a finite σ_0 . However, as implied above (see footnote 4), the two parameters σ_0 and q_{max} are strongly coupled, and either the temperature [16] or the surface tension of the system have to be changed to obtain σ_0 and q_{max} . By making an assumption (based on the observation and discussion above) that all liquids have, within uncertainty, similar σ_0 and q_{max} , and by fitting all data sets simultaneously, we obtain $\sigma_0 = 1.4 \pm 0.4 \text{ \AA}$ and $q_{\text{max}} = 0.152_{-0.06}^{+0.1} \text{ \AA}^{-1}$. Clearly the optimal q_{max} value from the fitting is significantly smaller than the value determined by molecular size R ($q_{\text{max}} \approx$

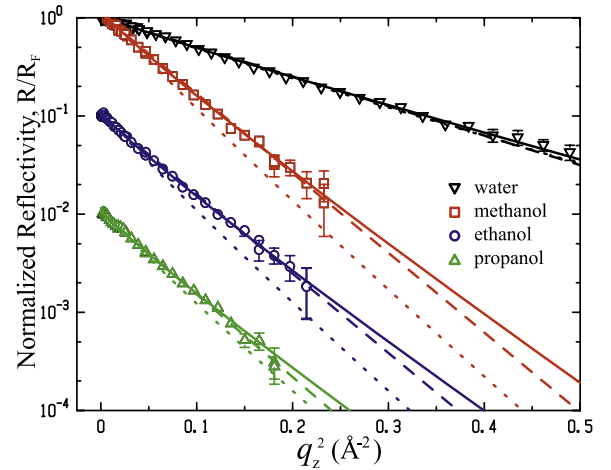


Figure 2. Normalized XR of the pure liquids versus q_z^2 . The dotted lines are the best fits using equation (3) with $q_{\text{min}} = q_z \Delta \beta / 2$ and a fixed $q_{\text{max}} = \pi/R$ varying only σ_0 , and the solid lines are obtained by varying q_{max} . The dashed lines are the best fits assuming a single parameter, q_z -independent σ'_{eff} .

1.63 and 1.01 \AA^{-1} for water and propanol, for example). This suggests capillary wave theory breaks down at an average length scale $l_r \approx \pi/q_{\text{max}} = 21_{-8.2}^{+13.2} \text{ \AA}$. A third way to fit the data is to simply assume q_z -independent σ'_{eff} , such as those shown by dashed lines in figure 2 demonstrating the q_z dependence of σ_{eff} is insignificant [18].

Figure 3(a) shows the normalized reflectivities from the water/ethanol mixtures. Reflectivities from the mixtures of methanol and propanol and their mixtures (not shown) are similar. The solid lines are the best fits to the data using equation (3) assuming a single parameter σ'_{eff} (q_z -independent). For all liquids, we carefully examined the region of the reflectivity near the critical angle and found excellent agreement with the average electron density of each mixture. We considered the atomic/molecular structure factor and found it has negligible effect on the extracted parameters. Also, we could not find any evidence of surface layering in the mixtures [24].

Figure 3(b) shows a compilation of all measured effective surface roughness values (σ_{eff}^2) versus the inverse of surface tension for each mixture, as indicated. The surface tension values of the mixtures are shown in the inset [24]. To a good approximation, all the measured roughness values fall on a linear curve (solid line) that confirms equation (4) within experimental error. This behavior strongly suggests the profile of the pure and liquid mixtures of small molecules is *predominantly* determined by surface tension (at a given temperature). From figure 3(b) we obtain values for σ_0 and for the slope $\Delta = k_B T \ln(q_{\text{max}}/q_{\text{min}}) / 2\pi$ as listed in table 1. The values of σ_0^2 , for both 8 and 16.2 keV are consistent within uncertainties. The difference between the values of Δ , is mainly due to different detector–slit configurations used at the two x-ray energies, yielding two different values for q_{min} . In the following, we make the assumption that σ_0 and q_{max} are, within uncertainties, the same for all liquids and mixtures. Although they should differ for the various liquids, the variation is most likely smaller than the experimental

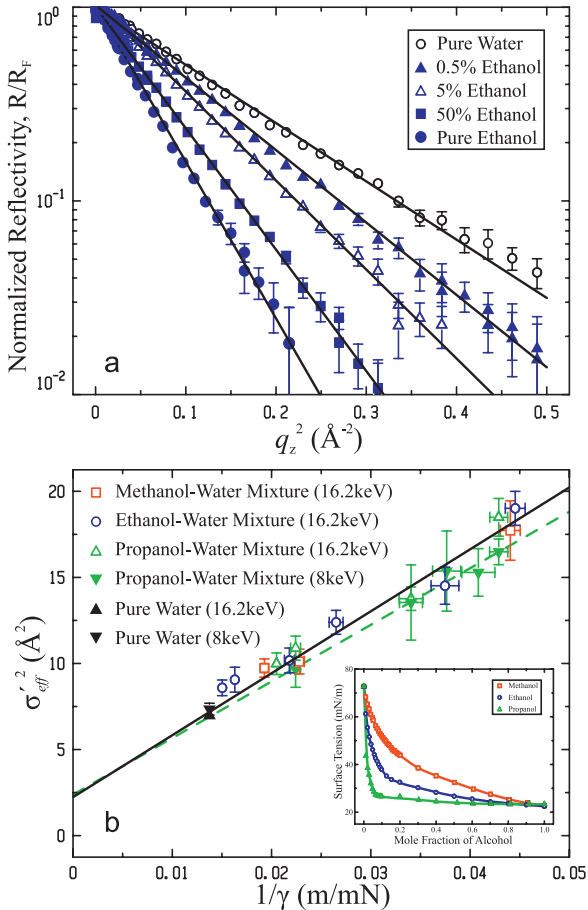


Figure 3. (a) Normalized x-ray reflectivity of the ethanol–water mixtures versus q_z^2 . The solid lines are linear fits to the (logarithm of) data yielding σ_{eff}^2 . (b) Compilation of σ_{eff}^2 values obtained from the analysis of the reflectivities versus the inverse of the surface tension. The solid line (16.2 keV) and dashed line (8 keV) are the best linear fits to the data. The inset in (b) shows the surface tension of water–alcohol mixtures with varying bulk concentrations.

uncertainty. This is rationalized based on the results of the pure alcohols above (figure 2) that yield within error the same σ_0 and q_{max} , although the three alcohols differ significantly in molecular size.

The value of the intrinsic roughness $\sigma_0 = 1.5 \pm 0.2 \text{ \AA}$ is very close to that of bond lengths in our systems (e.g. C–C and C–O with bond lengths 1.54 and 1.43 \AA , respectively). The theory for x-ray reflectivity above assumes the electron density is a continuum, but physically the electrons are concentrated around discrete nuclei, thereby giving rise to intrinsic roughness on the scale of atomic separations, hypothetically, even at zero temperature where all thermal motions are frozen. This is in agreement with the study of liquid alkanes, where it was found that $\sigma_0 = 1.1 \text{ \AA}$ and was correctly associated with interatomic C–C bond length [16]. Although in the present study of simple liquids, we find σ_0 is of the order of average interatomic distances, we do not rule out that, in more complex liquids, the intrinsic roughness may depend on molecular or aggregate size.

From the slope of the curve Δ in figure 3(b) we can estimate the value of q_{max} assuming $q_{\text{min}} = \langle q_z \rangle \Delta \beta / 2$, where

Table 1. Intercept σ_0^2 and slope Δ values obtained from linear fits to the data shown in figure 3 for two independent sets of experiments using 8 and 16.2 keV x-rays.

XR energy (keV)	σ_0^2 (\AA^2)	Δ ($\times 10^{-23}$ J)	q_{max} (\AA^{-1})	l_r (\AA)
16.2	$2.2^{+0.3}_{-0.2}$	360^{+42}_{-34}	$0.08^{+0.07}_{-0.03}$	40^{+28}_{-20}
8	$2.4^{+0.3}_{-0.3}$	329^{+35}_{-30}	$0.07^{+0.05}_{-0.03}$	48^{+29}_{-20}

$\langle q_z \rangle = 0.3 \text{ \AA}^{-1}$, at about the midpoint of the range over which the reflectivities were measured, as listed in table 1 (the slopes of the curves at 8 and 16.2 keV are slightly different due to different slit configurations). The corresponding l_r lengths are in fair agreement with the values obtained from the analysis of the pure liquids above (figure 2). Our view is that the value of l_r reflects bulk correlation length, a length scale below which capillary wave theory breaks down. Although thermal excitations may exist for $q \sim \pi/R$ and even at larger values, due to intermolecular vibrational states, these are of a different nature than those of capillary waves. Due to bulk short-range order, these may be more like optical phonons in solids, where it is common that their average amplitude (Debye–Waller factor) is only a few percent of interatomic distances, thus contributing negligibly compared to capillary waves. This is in agreement with the current view of capillary wave theories and simulations that assume fluctuations of the interface on length scales larger than the bulk correlation length [27]. The influence of the bulk properties on the surface behavior has been discussed theoretically and experimentally in the context of power spectra fluctuations of a liquid surface [28].

4. Summary

In the present synchrotron x-ray study, we systematically determined the profiles of the liquid/vapor interfaces of water and its mixtures with methanol, ethanol and propanol at a fixed temperature, with the premise that, while surface tension changes by mixing water with alcohols, the molecular size at the interface is as close as possible to that of the water molecule. We emphasize that the values we report for σ_0 and q_{max} , although expected to vary among the different liquids, are approximate and should be considered as a lower and an upper limit, respectively. We find that the intrinsic roughness for these simple liquids reflects interatomic distances setting a low limit to σ_0 . We also find that the upper wavevector cutoff for capillary waves (although with inherently large uncertainty) is appreciably smaller than that expected by assuming it is dominated by molecular diameter. This implies the breakdown of capillary wave theory at a few molecular diameters due to *rigidity* of the surface membrane over short length scales on the order of bulk correlation lengths.

Acknowledgments

We thank D S Robinson for technical support at the 6-ID beamline and A Travesset, B M Ocko and M Fukuto for helpful discussions. The MUCAT sector at the APS is supported by the

US DOE, Basic Energy Sciences, Office of Science, through Ames Laboratory under contract under contract no. DE-AC02-07CH11358. Use of the Advanced Photon Source is supported by the US DOE, Basic Energy Sciences, Office of Science, under contract no. W-31-109-Eng-38. DK acknowledges support from the Quantum Photonic Science Research Center (SRC) at Hanyang University and the World-Class University program.

References

- [1] Cahn J W and Hilliard J E 1958 *J. Chem. Phys.* **28** 258
- [2] Fisk S and Widom B 1969 *J. Chem. Phys.* **50** 3119
- [3] Buff F P, Lovett R A and Stillinger F H 1965 *Phys. Rev. Lett.* **15** 621
- [4] Weeks J D 1977 *J. Chem. Phys.* **67** 3106
- [5] Rowlinson J S and Widom B 1982 *Molecular Theory of Capillarity* (Oxford: Clarendon)
- [6] Beysens D and Robert M 1987 *J. Chem. Phys.* **87** 3056
- [7] Meunier J 1987 *J. Physique* **48** 1819
- [8] Sengers J V and van Leeuwen J M J 1989 *Phys. Rev. A* **39** 6346
- [9] Gelfand M P and Fisher M E 1990 *Physica A* **166** 1
- [10] Huang J S and Webb W W 1969 *J. Chem. Phys.* **50** 3677
- [11] Wu E S and Webb W W 1973 *Phys. Rev. A* **8** 2065
- [12] Braslau A *et al* 1988 *Phys. Rev. A* **38** 2457
- [13] Daillant J *et al* 1989 *Europhys. Lett.* **8** 453
- [14] Schwartz D K *et al* 1990 *Phys. Rev. A* **41** 5687
- [15] Sanyal M K *et al* 1991 *Phys. Rev. Lett.* **66** 628
- [16] Ocko B M *et al* 1994 *Phys. Rev. Lett.* **72** 242
- [17] Fukuto M *et al* 1998 *Phys. Rev. Lett.* **81** 3455
- [18] Pershan P S 2000 *Colloids Surf.* **171** 149
- [19] Shpyrko O *et al* 2004 *Phys. Rev. B* **69** 245423
- [20] Fukuto M *et al* 2006 *Phys. Rev. E* **74** 031607
- [21] Als-Nielsen J and Pershan P S 1983 *Nucl. Instrum. Methods* **208** 545
- [22] Sinha S K *et al* 1988 *Phys. Rev. B* **38** 2297
- [23] Bu W and Vaknin D 2009 unpublished
- [24] Sung J, Park K and Kim D 2005 *J. Phys. Chem. B* **109** 18507
- [25] Vaknin D 2003 *Characterization of Materials* vol 2, ed E N Kaufmann (New York: Wiley) p 1027
- [26] Bu W, Vaknin D and Travasset A 2006 *Langmuir* **22** 5673
- [27] Mecke K and Dietrich S 1999 *Phys. Rev. E* **59** 6766
Blokhuis E, Groenewold J and Bedeaux D 1999 *Mol. Phys.* **96** 397
Vink R L C, Horbach J and Binder K 2005 *J. Chem. Phys.* **122** 134905
Tarazona P, Checa R and Chacon E 2007 *Phys. Rev. Lett.* **99** 196101
- [28] Bouchiat M A and Meunier J 1971 *J. Physique* **32** 561